
GRAPHGPT: GRAPH LEARNING WITH GENERATIVE PRE-TRAINED TRANSFORMERS

Qifang Zhao, Weidong Ren, Tianyu Li, Xiaoxiao Xu & Hong Liu

Alibaba Group, Hangzhou, China

{james.zqf, renweidong.rwd}@alibaba-inc.com

{qianchuan.lty, xiaoxiao.xu, liuhong.liu}@alibaba-inc.com

ABSTRACT

We introduce *GraphGPT*, a novel model for Graph learning by self-supervised Generative Pre-training Transformers. Our model transforms each graph or sampled subgraph into a sequence of tokens representing the node, edge and attributes reversibly using the Eulerian path first. Then we feed the tokens into a standard transformer decoder and pre-train it with the next-token-prediction (NTP) task. Lastly, we fine-tune the GraphGPT model with the supervised tasks. This intuitive, yet effective model achieves superior or close results to the state-of-the-art methods for the graph-, edge- and node-level tasks on the large scale molecular dataset PCQM4Mv2, the protein-protein association dataset ogbl-ppa and the ogbn-proteins dataset from the Open Graph Benchmark (OGB). Furthermore, the generative pre-training enables us to train GraphGPT up to 400M+ parameters with consistently increasing performance, which is beyond the capability of GNNs and previous graph transformers. The source code and pre-trained checkpoints will be released soon¹ to pave the way for the graph foundation model research, and also to assist the scientific discovery in pharmaceutical, chemistry, material and bio-informatics domains, etc.

1 INTRODUCTION

After the breakthrough of deep learning in 2012 (Krizhevsky et al., 2012), the computer vision (CV) and natural language processing (NLP) communities prosper till now. Graph community also benefits from this paradigm shifting from traditional machine learning to deep learning with the proposal of various graph neural networks (GNNs) (Kipf & Welling, 2017; Hamilton et al., 2017; Zhang & Chen, 2018; Wu et al., 2020).

Nowadays, both CV (Dosovitskiy et al., 2021; Liu et al., 2021) and NLP (Devlin et al., 2019; Radford et al., 2018) adopt the transformer backbone as the canonical architecture, and expand the model scale to billions or even hundreds of billions of parameters (Liu et al., 2021; Brown et al., 2020). These large models are trained with web-scale data (Schuhmann et al., 2022; Touvron et al., 2023), and achieve performance superior to human beings in many benchmark datasets (Deng et al., 2009; Wang et al., 2019b;a). These works also boost the commercial applications like Midjourney (Midjourney, 2023) and ChatGPT (Open-AI, 2023). However, GNNs are still suffering from the over-smoothing (Rusch et al., 2023) and over-squashing (Alon & Yahav, 2021) problems, which limit them to be expanded to larger scale and trained with larger amount of graph data.

In recent years, there are many works that tried to utilize transformers to model the graph data, and obtained good performance in certain graph datasets (Ying et al., 2021; Kim et al., 2022; Luo et al., 2023; Müller et al., 2023). Nevertheless, they often use complex tricks to handcraft features to encode structure information explicitly, and then inject them into either the input or the attention layers. These tricks restrain the generalization beyond specific datasets. In addition, these graph transformers (GTs) often perform well in graph-level tasks, but not applicable for the edge-/node-level tasks (Müller et al., 2023). Last but not least, self-supervised generative pre-training is the key of the success of GPTs (Radford et al., 2018), but it is hardly incorporated in the GTs (Min et al., 2022; Müller et al., 2023).

¹<https://github.com/alibaba/graph-gpt>

In this work, we propose *GraphGPT*, a novel model for graph learning. It consists of three non-trivial components: 1) transforming the (sub)graphs into a reversible sequence of tokens via the Eulerian path, 2) pre-training a transformer decoder using the NTP task, and 3) fine-tuning the transformer with any supervised graph tasks. GraphGPT is able to overcome the disadvantages of GNNs and Graph Transformers, and obtains state-of-the-art (SOTA) results in graph-/edge-/node-level tasks. Our contributions are summarized as follows:

- GraphGPT employs (semi-)Eulerian path² to transform the graphs into the sequences of tokens, which ensures the transformation is lossless, reversible and optimal. Together with subgraph sampling and node identity encoding techniques, we can transform graphs of various sizes into sequences of tokens.
- GraphGPT is generatively pre-trained with the NTP task, which brings 3 advantages: *a)* learning the graph’s structural and semantic information without relying on handcrafted features or tailored transformer architectures; *b)* scaling up to 400M+ parameters with consistent performance improvement; *c)* possessing the capability to generate graphs.
- GraphGPT utilizes a novel approach to format graph-/edge-/node-level tasks, making them compatible with the transformer decoder architecture and enabling them to fully benefit from the generative pre-training.
- Through extensive experiments on the public OGB datasets, GraphGPT achieves SOTA results in graph-level and edge-level tasks, and the performance in node-level tasks approaches the SOTA level.

2 APPROACH

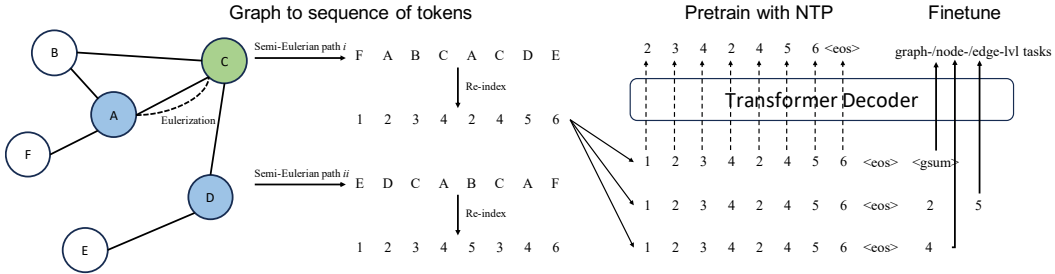


Figure 1: Model overview. The left part shows the procedure to convert a (sub)graph into a sequence of tokens. The dashed line indicates the duplicated edge added to the original graph to make it (semi-)Eulerian. The right part shows the pre-training with the self-supervised NTP task and fine-tuning on the supervised graph-/edge-/node-level tasks. We use edge (A, D) as an example for the edge-level task, and node C for the node-level task.

2.1 OVERVIEW

In our GraphGPT model, we transform the given graph into a sequence of tokens in a reversible manner, ensuring that the graph and the resulting sequence are equivalent. Then we utilize a standard transformer backbone, such as Llama from Touvron et al. (2023), to process the sequence data and train it using the self-supervised NTP task. Finally, we fine-tune the transformer with the supervised tasks such as graph classification/regression, link prediction and node classification.

2.2 GRAPH TO SEQUENCE OF TOKENS

In this section, we show how to convert a graph into a sequence of tokens. For small graphs, *e.g.*, molecular graphs, we convert them to sequences as in Sec. 2.2.1. Big graphs, *e.g.*, graphs with hundreds of thousands of nodes, millions or even billions of edges and many node or edge attributes, are

²For a quick recap, a graph with every node of even degree is Eulerian, and with exactly two nodes of odd degree is semi-Eulerian.

processed differently. We first sample subgraphs (see Sec. 2.2.2) with the node identity information preserved (see Sec. 2.2.3), and then transform them into sequences in accordance with Sec. 2.2.1.

2.2.1 SERIALIZING GRAPHS WITH (SEMI-)EULERIAN PATH

We aim to find a lossless and reversible method to serialize (sub)graphs into sequences of tokens. This requires all the nodes and edges shall be represented in the sequence. Therefore, a path that transverses all the edges and nodes at least once would be a candidate.

This type of path is studied in the literature as the Chinese Postman Problem six decades ago, and it can be solved in polynomial time (Mei-Ko, 1962; Edmonds & Johnson, 1973). In precise, if the graph has a (semi-)Eulerian path, that path is an optimal solution. Otherwise, we need to find the smallest number of existing edges to duplicate so that the resulting multigraph does have an (semi-)Eulerian path.

Given a (sub)graph, we can easily check whether it is (semi-)Eulerian (West et al., 2001). If it is not, we can always convert it to be a (semi-)Eulerian graph by duplicating some existing edges, which is defined as Eulerization (Edmonds & Johnson, 1973; Daubechies & Hughes, 2009). Then, we can obtain the (semi-)Eulerian path for the given graph. Since there are often more than one path for the (semi-)Eulerian graph, we randomly sample one of the paths for training. This can be regarded as data augmentation, which has been proven to be very helpful in CV (Perez & Wang, 2017).

We then re-index the nodes with $1, 2, \dots, n$ according to the order of their appearance in the path, where n is the total number of nodes. As in the example of the Fig. 1, n of the path i is 6, and the node F is re-indexed as '1' and A is re-indexed as '2'.

For graphs with node attributes, and edge weights/attributes/directions (*i.e.*, directed graphs), we represent the discrete attributes with tokens, and split the continuous numbers into individual digits as the tokens. We assign two tokens to represent the incoming and outgoing edge directions respectively. The tokens of a node's attributes are appended right after the node token (*e.g.*, '1', '2'), and the tokens of the edge's attributes are put in between the source and destination nodes (see Appendices D to F for detailed examples).

For the graph with disconnected components, we connect them by adding edges between the randomly picked nodes from different components. We use the token `<edge_jump>` as those edges' attributes.

We claim that the conversion of the graph to the sequence of tokens is lossless and reversible, because one can always recover the original graph by connecting the adjacent tokens. For example, in the sequence i of Fig. 1, by linking '1' to '2', '2' to '3' and so on, we obtain all the edges as ensured by the Eulerian Path Theorem. With all the edges, we are able to construct a graph equivalent to the original one except for the notations of the nodes. More rigorously, they are isomorphic (Grohe & Schweitzer, 2020).

2.2.2 SUBGRAPH SAMPLING

Serializing a large graph as in Sec. 2.2.1 leads to an extremely long sequence, which cannot be fed into the transformer. To tackle the problem, one way is to convert the whole graph into a sequence first, and then divide it into segments that can be fed into the transformer. The other way involves sampling subgraphs and then converting them into sequences. Both Eulerizing a big graph and finding its Eulerian path are quite time-consuming. Additionally, it causes the inconsistency between the sequences in pre-training and fine-tuning. Therefore, we adopt the second way to serialize a large graph.

To be more specific, we sample a subgraph randomly around the central edge or node using the ShaDowKHop sampler introduced in Zeng et al. (2021). To ensure the resulting sequences to fit into the context window, we pre-calculate the depth and number of neighbors of the ShaDowKHop sampler. They vary across different datasets and context windows (see App. A.1 for more).

2.2.3 NODE IDENTITY ENCODING

When sampling subgraphs from a large graph, we need to preserve the nodes’ global identity, otherwise much information will be lost. One straightforward method is to represent each node as a unique token in the transformer’s vocabulary, *i.e.*, to encode each node with a learnable embedding vector. However, when the number of nodes in the graph is huge, the vocabulary size becomes enormous, causing the model size to increase significantly, and making the training difficult.

To avoid the problem, we propose to encode each node with multiple tokens. For example, given a graph with 10 billion (10^{10}) nodes, we can encode each node uniquely with two tokens, and each token ranges from 1 to 10^5 . As a result, this encoding would utilize 10^5 instead of previous 10^{10} tokens in the vocabulary. It can be implemented with METIS (Karypis & Kumar, 1997) to partition the graph into 10^5 partitions, and each partition roughly has 10^5 nodes. To further reduce the vocabulary size, we can encode each node with more tokens. For instance, encoding with five tokens results in a vocabulary size of 100. However, note that encoding each node with more tokens would increase the length of the resulting graph sequence.

The above encoding schema is in analogy with the coding of characters in computing. We can encode any characters with variable numbers of bytes in utf-8 (Allen et al., 2012, Chapter 2), and the resulting vocabulary is 256, which is the count of all possible bytes.

Through encoding each node uniquely with multiple tokens, we guarantee that the nodes’ identity information is preserved during the subgraph extraction process. We show later in the ablation study in Sec. 3.5.3 that it does improve the results.

2.3 MODELING WITH THE TRANSFORMER DECODER

In this section, we show that we can model various graph tasks with the pre-training and fine-tuning paradigm using the transformer decoder architecture on the graph sequence of tokens.

2.3.1 PRE-TRAINING WITH THE NTP TASK

Self-supervised pre-training has been shown very beneficial for various NLP tasks (Devlin et al., 2019; Radford et al., 2019). The next-token-prediction (NTP) and masked-token-prediction tasks are two widely adopted self-supervised tasks. The NTP helps various models attain the SOTA results in many NLP tasks, and it enables the resulting model with strong generation capability (Brown et al., 2020). So we choose the NTP as our pre-training task.

As shown in the right part of Fig. 1, the NTP predicts the next node to connect in the context of graph sequence. The next node can be a new node, one of the previous nodes, or the end (*i.e.*, the $\langle \text{eos} \rangle$ token). For example, in the semi-Eulerian path i , given the node sequence ‘1’, ‘2’ and ‘3’, we predict that the next node is a new node and assign the notation ‘4’ to it. Subsequently, we predict to connect to the previous node ‘2’, and so on. Finally, after we arrive at node ‘6’, we predict the end. In the presence of node and edge attributes, the NTP also predicts the corresponding discretized tokens encoded in the graph sequence.

2.3.2 FINE-TUNING ON DOWNSTREAM GRAPH TASKS

As shown in Fig. 1, we append a special token $\langle \text{gsum} \rangle$ at the end of the graph sequence, and feed its embedding output to a multilayer perceptron (MLP) for the supervised graph-level task. The parameters of the transformer are initialized from the pre-trained checkpoint, while the MLP layers are randomly initialized. All the parameters are updated during the fine-tuning stage.

For the supervised edge-level task, we append the tokens of the source and destination nodes of the target edge at the end of the sequence. The output of the last token from the transformer is then fed to a MLP layer for the task. Similarly, for the node-level task, we append the target node’s token at the end of the graph sequence and utilize its output for the task’s MLP layer.

By reformatting the graph-/edge-/node-level tasks as above, our pre-training and fine-tuning are aligned in an elegant manifestation. The alignment allows the fine-tuning tasks to better exploit the competency of pre-training, which is verified by many NLP literature (Brown et al., 2020; Wei et al., 2021). Moreover, one can eliminate the task-specific MLP layer and convert the supervised

task labels into tokens. Then the model is fine-tuned to generate these tokens, in analogy to the approach employed by GPT-3 for many NLP tasks (Brown et al., 2020).³

3 EXPERIMENTS

3.1 DATASETS

Applying AI to accelerate scientific discovery has been prevailing recently (Hassabis, 2023), which motivates us to validate our proposal on the large-scale graph datasets from physical, chemical, pharmaceutical and bio-informatics domains. Also, we aim to demonstrate that our GraphGPT is applicable in the mainstream graph tasks, including graph-/edge-/node-level tasks. Therefore, we choose PCQM4Mv2 and ogbg-molpcba for the graph-level task, and ogbl-ppa for the edge-level task and ogbn-proteins for the node-level task (Hu et al., 2020; 2021). Their statistics are shown in Tab. 8 of App. A.

The PCQM4Mv2 is a quantum chemistry dataset of more than 3.7 million small organic molecules from the PubChemQC project (Nakata & Shimazaki, 2017). The ogbg-molpcba is a much smaller molecular dataset (Wu et al., 2017). In these 2D molecular graphs, nodes are atoms, and edges are chemical bonds. The node attributes are 9-dimensional, containing atomic number, chirality and other atom features. The edge attributes are 3-dimensional, *i.e.*, bond type, bond stereochemistry and conjugation.

In the ogbl-ppa dataset, the nodes are proteins from 58 different species, and edges represent biologically meaningful associations between proteins (Szklarczyk et al., 2019). It is a large graph of over 30 million edges.

The ogbn-proteins dataset is an undirected, weighted, and typed dense graph. The nodes are proteins from 8 species, and the edges’ 8-dimensional attributes represent 8 types of association strengths. It has nearly 40 million edges. See more implementation details in App. C.

3.2 GRAPH-LEVEL TASKS

Table 1: Results of the graph classification task on the ogbg-molpcba dataset. All the baseline results are from the OGB leaderboard and the corresponding papers. The best results are in bold, and second-best are underlined.

Models	Average Precision (AP)		Params
	Test	Valid	
GCN	0.2020±0.0024	0.2059±0.0033	0.57M
GIN	0.2266±0.0028	0.2305±0.0027	1.92M
GINE+bot	0.2994±0.0019	<u>0.3094±0.0023</u>	5.51M
Nested GIN+virtual node	<u>0.3007±0.0037</u>	0.3059±0.0056	44.19M
PDF	0.3031±0.0026	0.3115±0.0020	3.84M
GraphGPT-mini	0.2385±0.0012	0.2777±0.0017	4.48M
GraphGPT-base	0.2517±0.0041	0.2857±0.0033	114.12M
GraphGPT-large	0.2722±0.0022	0.2966±0.0027	403.84M

For the two molecular datasets, the tasks are to predict quantum chemical property only from 2D molecular graphs without their 3D equilibrium structures, which is practically favorable. We predict 128 binary molecular properties for ogbg-molpcba and the HOMO-LUMO gap for PCQM4Mv2.

We experiment 3 models of parameters from 4.48M to 403.84M for the ogbg-molpcba dataset. We pre-train the models with 16B tokens, and then fine-tuned for 10 epochs. The results from the epoch that maximizes the validation metric are reported in Tab. 1.

Our GraphGPT produces results much better than the powerful GNNs like GCN and GIN (Kipf & Welling, 2017; Xu et al., 2019). Our results also approach the SOTA from those sophisticated

³We do not investigate it in this work, and leave it for future study.

GNNs. In addition, GraphGPT yields consistently improved results as we increase the model size up to 400M. This verifies that GraphGPT does not suffer from the over-smoothing or over-squashing problems common in GNNs. It suggests that GraphGPT can perform even better if pre-trained with more data and more parameters.

Table 2: Results of the graph regression task on the PCQM4Mv2 dataset. The metric is mean absolute error (MAE), the smaller the better. We highlight the results that do not use 3D data.

Models		Use 3D	MAE		Params
			Valid	Test	
GNNs	GCN	✗	0.1379	0.1398	2.0M
	GIN	✗	0.1195	0.1218	3.8M
	GCN-VN	✗	0.1153	0.1152	4.9M
	GIN-VN	✗	0.1083	0.1084	6.7M
GTs	TokenGT	✗	0.0910	0.0919	48.5M
	Graphformer	✗	0.0864	N/A	48.3M
	Transformer-M	✓	0.0772	0.0782	69.0M
	Uni-Mol+	✓	0.0693	0.0705	770.3M
Ours	GraphGPT	✗	0.0875	N/A	49.7M

As for PCQM4Mv2, we compare to two GTs that do not utilize the molecular 3D data, *i.e.*, TokenGT and Graphformer (Kim et al., 2022; Ying et al., 2021). We configure our transformer backbone the same as theirs for a fair comparison. The resulting model has 49.7M parameters, and is pre-trained with about 49.5B tokens.

The TokenGT uses the vanilla transformer backbone, and it serializes the graph into tokens by directly unfolding all the nodes and edges. The serialization method prohibits it from being self-supervised pre-trained. TokenGT also supplements the inputs with handcrafted structural features.

The Graphformer transforms the graph into the sequence of tokens using nodes only. The structural information possessed in the edges are completely lost in the input sequence, so Graphformer has to add them back through modifying the transformer’s attention layers and enhancing the inputs with sophisticated tricks like centrality encoding and spatial encoding to handcraft structural information. Same as TokenGT, Graphformer cannot adopt self-supervised pre-training.

In contrast, our GraphGPT does not require any handcrafted features, and obtains better results than TokenGT on the valid dataset, *i.e.*, 0.0875 versus 0.0910. Our result is comparable to Graphformer. What’s more, GraphGPT surpasses all the GNNs by a large margin. The exceptional performance of GraphGPT implies that our lossless serialization and the self-supervised generative pre-training enable the model to fully capture the graph’s structural and semantic information. We are pre-training larger GraphGPT with more compute budget in order to attain better results.

3.3 EDGE-LEVEL TASKS

The edge-level task of the dataset ogbl-ppa is link prediction. We use two tokens for the node identity encoding introduced in Sec. 2.2.3. Specifically, we use the species to partition the nodes, so the first token represents the species, and the second is the local indices of proteins inside each species (see App. E for details).

We experiment 5 different model sizes ranging from 14.75M to 444.92M, and report 3 of them in Tab. 3 (see App. E for more). GraphGPT-mini/base/large are pre-trained with 25.6B/39B/50B tokens respectively, and then fine-tuned with the classification task. The fine-tuning data consists of subgraphs induced by the positive edges for training and equal negative edges randomly sampled.

As in Tab. 3, GraphGPT performs much better than all kinds of models, including GNNs, Heuristic and Latent Factor models. Our smallest model outperforms the strong GNNs like GCN, GraphSAGE and SEAL a lot (Kipf & Welling, 2017; Hamilton et al., 2017; Zhang & Chen, 2018). Our best result 67.15 surpasses the current SOTA 63.22 by a large margin.

AGDN (Sun et al., 2020), the largest GNN in the leaderboard, has only 36.9M parameters. The prevailing GNNs like GCN, GraphSAGE and SEAL have less than 1M parameters. They cannot be further scaled up to achieve better results due to the over-smoothing and over-squashing problems. In contrast, GraphGPT is able to scale up to 400M+ with consistently increasing performance. This motivates further study on larger models and more data with more compute budget.

What’s more, previously no GTs are listed in the ogbl-ppa’s leaderboard, and we show that transformer based models can excel in edge-level tasks.

Table 3: Results of the link prediction task on the ogbl-ppa dataset.

Models		HR@100 (%)		Params
		Test	Valid	
Heuristic	Common Neighbor	27.65±0.00	28.23±0.00	0
	Adamic Adar	32.45±0.00	32.68±0.00	0
	Resource Allocation	49.33±0.00	47.22±0.00	0
Latent Factor	DeepWalk	28.88±1.53	-	150.14M
	Matrix Factorization	32.29±0.94	32.28±4.28	147.66M
GNN	GCN	18.67±1.32	18.45±1.40	0.28M
	GraphSAGE	16.55±2.40	17.24±2.64	0.42M
	SEAL	48.80±3.16	51.25±2.52	0.71M
	AGDN	41.23±1.59	43.32±0.92	36.90M
	SIEG	63.22±1.74	65.33±2.34	1.99M
GraphGPT (Ours)	mini	55.56±1.14	54.87±0.66	14.75M
	base	64.98±1.73	66.68±1.33	144.93M
	large	67.15±1.36	68.60±1.40	444.92M

3.4 NODE-LEVEL TASKS

The task of the ogbn-proteins dataset is to predict 112 binary labels of proteins that each indicates the presence of one type of function. The node identity is encoded with two tokens similar to the ogbl-ppa in Sec. 3.3 (see App. F for details).

We pre-train 5 different models that scale from 10.76M to 428.94M with 51.2B tokens, and then fine-tune them for 16 epochs. We pick the 3 consecutive epochs that maximize the metric of valid data and then calculate the mean and variance. We report the results of 3 models in Tab. 4.

For this dataset, GNNs usually use random partition (Li et al., 2020) to sample subgraphs. The resulting subgraphs usually have more than 20,000 nodes and 1 million edges. In contrast, our subgraphs usually have about 10 nodes and 20 edges, because we limit the transformers’ context window to be 256. It is remarkable that GraphGPT’s results surpass GCN and GraphSAGE, and approach the SOTA with such a small neighborhood to gather information. We hypothesize that during the pre-training, the global structural and semantic information of the big graph have been encoded in the node tokens’ embeddings and the transformer’s parameters.

GNNs in the leaderboard are very small. For example, GCN and GraphSAGE has 0.1M to 0.2M parameters, and even DeeperGCN does not exceed 2.37M (Li et al., 2020). The largest GNN model RevGNN-wide has 68M parameters (Li et al., 2021). In contrast, our GraphGPT-large has 400M+ parameters and can be well trained. Compared to the only transformer based model UniMP in the leaderboard (Shi et al., 2020), GraphGPT is able to train much larger transformers and attains improved results.

Despite of the fine performance of GraphGPT, the small context window may restrain its capability. Techniques like Flash Attention (Dao et al., 2022) and Positional Interpolation (Chen et al., 2023) can be utilized to make the context window much longer.⁴

⁴We experimented with the context window of 1024, and observed some gains.

Table 4: Results of the node classification task on the ogbn-proteins dataset.

Models	ROC-AUC (%)		Params
	Test	Valid	
GCN	72.51±0.35	79.21±0.18	0.10M
GraphSAGE	77.68±0.20	83.34±0.13	0.19M
DeeperGCN	85.80±0.17	91.06±0.16	2.37M
UniMP	86.42±0.08	91.75±0.06	1.91M
RevGNN-wide	<u>88.24±0.15</u>	<u>94.50±0.08</u>	68.47M
GIPA (Wide&Deep)	89.17±0.07	94.72±0.20	17.44M
GraphGPT-mini	75.61±1.37	80.47±0.94	10.76M
GraphGPT-base	83.37±0.15	87.68±0.25	132.94M
GraphGPT-large	84.80±0.18	89.35±0.24	428.94M

3.5 ABLATION STUDY

We present the ablation study on three key ingredients of GraphGPT, *i.e.*, pre-training, node re-indexing and node identity encoding.

3.5.1 PRE-TRAINING

Pre-training with the NTP task is the key to the success of our GraphGPT. Experiment results on graph/edge/node-level tasks in Tab. 5 show that pre-training can boost the performance a lot. The lift of metrics ranges from 30% to 100%. This implies that pre-training enables the model to understand both the graph structure and the semantics possessed in the node and edge attributes.

Table 5: Ablation study of pre-training on the datasets of various types of tasks.

Task Type	Datasets	Params	Metrics	Pre-training	Test	Valid
Graph	ogbg-molpcba	4.48M	AP	✗	0.1280	0.1331
				✓	0.2385	0.2777
	PCQM4Mv2	49.7M	MAE	✗	N/A	0.1086
				✓	N/A	0.0875
Edge	ogbl-ppa	14.75M	HR@100	✗	41.28	40.14
				✓	55.56	54.87
Node	ogbn-proteins	10.76M	ROC-AUC	✗	57.52	61.19
				✓	75.61	80.47

3.5.2 NODE RE-INDEXING

As shown in Fig. 1, we re-index the nodes according to their order in the (semi-)Eulerian path. We conduct experiments using the ogbg-molpcba dataset to assess its effectiveness. As shown in Tab. 6, node re-indexing improves the downstream tasks for different model sizes, although it increases the pre-training loss. This is because node re-indexing can be regarded as data augmentation. It prevents the model from memorizing the unimportant information of the graph, *i.e.*, the notation of the nodes, and leads to better generalization performance. In addition, the re-indexing allows us to restrict the decoding space of node tokens when generating graphs with GraphGPT.

3.5.3 NODE IDENTITY ENCODING

As illustrated in Sec. 2.2.3, we encode each node in a big graph uniquely with multiple tokens. Here we show its importance for edge-/node-level tasks. We use GraphGPT-mini to conduct the ablation

Table 6: Ablation study of node re-indexing on the ogbg-molpcba dataset with two model sizes.

Params	Metrics	Re-index	Pre-training Loss	Test	Valid
114.12M	AP	✗	0.0689	0.2270	0.2621
		✓	0.0750	0.2517	0.2857
4.48M	AP	✗	0.0844	0.2310	0.2525
		✓	0.0874	0.2385	0.2777

study to save time and compute budget. Node identity encoding can obviously improve the results as in Tab. 7. For more details, see appendices A and E.

Table 7: Ablation study of node identity encoding on the ogbl-ppa and ogbn-proteins datasets.

Task Type	Datasets	Params	Metrics	Node ID encoding	Test	Valid
Edge	ogbl-ppa	14.75M	HR@100	✗	44.38	45.08
				✓	55.56	54.87
Node	ogbn-proteins	10.76M	ROC-AUC	✗	60.22	65.66
				✓	75.61	80.47

4 RELATED WORKS

Graph Neural Networks (GNNs) GNNs have been dominating the graph learning in the past decades. They have many variants, and gain excellent performance in various graph tasks (Wu et al., 2020). However, most GNNs suffer from the over-smoothing and over-squashing problems, which restrict them from scaling up (Rusch et al., 2023; Alon & Yahav, 2021).

Graph Transformers (GTs) Inspired by the success of transformers in NLP and CV, graph community starts to embrace transformer architectures in recent years (Ying et al., 2021; Rampásek et al., 2022; Müller et al., 2023). The various GTs have attained some good results, especially in graph-level tasks with large-scale datasets (Müller et al., 2023). Nevertheless, they have to employ handcrafted features or GNN modules to encode the structure information in the inputs (Ying et al., 2021; Kim et al., 2022), and/or in the self-attention layers (Ying et al., 2021; Chen et al., 2022; Luo et al., 2023). In addition, they mostly adopt the transformer encoder instead of the decoder, preventing them from being pre-trained in a self-supervised manner.

Pre-training and fine-tuning After the invention of the transformer (Vaswani et al., 2017), the self-supervised pre-training and supervised fine-tuning paradigm starts to flourish in NLP and brings significant improvements across various tasks (Devlin et al., 2019; Radford et al., 2018). Pre-training with web-scale text data (Brown et al., 2020) and followed by instruction tuning (Wei et al., 2021) or reinforcement learning from human feedback (Ouyang et al., 2022) advances the paradigm and boosts the performance even further. In CV, pre-training with the large scale supervised datasets and fine-tuning on the small datasets gains much success, which is termed as transfer learning (Yosinski et al., 2014). Recently, MAE from He et al. (2022) shows that self-supervised pre-training by predicting large portion of masked image patches can also attain SOTA results.

5 CONCLUSIONS

We propose the novel model GraphGPT that can be adapted for the graph-/edge-/node-level tasks, and it can attain SOTA or close to SOTA results. With GraphGPT, we train large models of up to hundreds of millions parameters, and observe consistent performance increase. GraphGPT has the potential to be scaled up to hundreds of billions parameters, and can be aligned or integrated with large language models. For a comprehensive understanding of GraphGPT, we discuss its limitations in App. G.

REFERENCES

- Julie D Allen, Deborah Anderson, Joe Becker, Richard Cook, Mark Davis, Peter Edberg, Michael Everson, Asmus Freytag, Laurentiu Iancu, Richard Ishida, et al. *The unicode standard*. Citeseer, 2012.
- Uri Alon and Eran Yahav. On the bottleneck of graph neural networks and its practical implications. In *International Conference on Learning Representations*, 2021. URL <https://openreview.net/forum?id=i800PhOCVH2>.
- Tom Brown, Benjamin Mann, Nick Ryder, Melanie Subbiah, Jared D Kaplan, Prafulla Dhariwal, Arvind Neelakantan, Pranav Shyam, Girish Sastry, Amanda Askell, et al. Language models are few-shot learners. *Advances in neural information processing systems*, 33:1877–1901, 2020.
- Dexiong Chen, Leslie O’Bray, and Karsten M. Borgwardt. Structure-aware transformer for graph representation learning. In Kamalika Chaudhuri, Stefanie Jegelka, Le Song, Csaba Szepesvári, Gang Niu, and Sivan Sabato (eds.), *International Conference on Machine Learning, ICML 2022, 17-23 July 2022, Baltimore, Maryland, USA*, volume 162 of *Proceedings of Machine Learning Research*, pp. 3469–3489. PMLR, 2022. URL <https://proceedings.mlr.press/v162/chen22r.html>.
- Shouyuan Chen, Sherman Wong, Liangjian Chen, and Yuandong Tian. Extending context window of large language models via positional interpolation. *CoRR*, abs/2306.15595, 2023. doi: 10.48550/arXiv.2306.15595. URL <https://doi.org/10.48550/arXiv.2306.15595>.
- Tri Dao. Flashattention-2: Faster attention with better parallelism and work partitioning. *CoRR*, abs/2307.08691, 2023. doi: 10.48550/ARXIV.2307.08691. URL <https://doi.org/10.48550/arXiv.2307.08691>.
- Tri Dao, Dan Fu, Stefano Ermon, Atri Rudra, and Christopher Ré. Flashattention: Fast and memory-efficient exact attention with io-awareness. *Advances in Neural Information Processing Systems*, 35:16344–16359, 2022.
- Ingrid Daubechies and Shannon Hughes. Graph theory, 2009. URL http://web.math.princeton.edu/math_alive/5/Notes1.pdf.
- Jia Deng, Wei Dong, Richard Socher, Li-Jia Li, Kai Li, and Li Fei-Fei. Imagenet: A large-scale hierarchical image database. In *2009 IEEE Computer Society Conference on Computer Vision and Pattern Recognition (CVPR 2009), 20-25 June 2009, Miami, Florida, USA*, pp. 248–255. IEEE Computer Society, 2009. doi: 10.1109/CVPR.2009.5206848. URL <https://doi.org/10.1109/CVPR.2009.5206848>.
- Tim Dettmers, Mike Lewis, Sam Shleifer, and Luke Zettlemoyer. 8-bit optimizers via block-wise quantization. In *The Tenth International Conference on Learning Representations, ICLR 2022, Virtual Event, April 25-29, 2022*. OpenReview.net, 2022. URL <https://openreview.net/forum?id=shpkpVXzo3h>.
- Jacob Devlin, Ming-Wei Chang, Kenton Lee, and Kristina Toutanova. BERT: pre-training of deep bidirectional transformers for language understanding. In Jill Burstein, Christy Doran, and Thamar Solorio (eds.), *Proceedings of the 2019 Conference of the North American Chapter of the Association for Computational Linguistics: Human Language Technologies, NAACL-HLT 2019, Minneapolis, MN, USA, June 2-7, 2019, Volume 1 (Long and Short Papers)*, pp. 4171–4186. Association for Computational Linguistics, 2019. doi: 10.18653/v1/n19-1423. URL <https://doi.org/10.18653/v1/n19-1423>.
- Alexey Dosovitskiy, Lucas Beyer, Alexander Kolesnikov, Dirk Weissenborn, Xiaohua Zhai, Thomas Unterthiner, Mostafa Dehghani, Matthias Minderer, Georg Heigold, Sylvain Gelly, Jakob Uszkoreit, and Neil Houlsby. An image is worth 16x16 words: Transformers for image recognition at scale. In *9th International Conference on Learning Representations, ICLR 2021, Virtual Event, Austria, May 3-7, 2021*. OpenReview.net, 2021. URL <https://openreview.net/forum?id=YicbFdNTTy>.

-
- Jack Edmonds and Ellis L Johnson. Matching, euler tours and the chinese postman. *Mathematical programming*, 5:88–124, 1973.
- Matthias Fey and Jan E. Lenssen. Fast graph representation learning with PyTorch Geometric. In *ICLR Workshop on Representation Learning on Graphs and Manifolds*, 2019.
- Elias Frantar, Saleh Ashkboos, Torsten Hoefer, and Dan Alistarh. GPTQ: accurate post-training quantization for generative pre-trained transformers. *CoRR*, abs/2210.17323, 2022. doi: 10.48550/ARXIV.2210.17323. URL <https://doi.org/10.48550/arXiv.2210.17323>.
- Martin Grohe and Pascal Schweitzer. The graph isomorphism problem. *Communications of the ACM*, 63(11):128–134, 2020.
- Aric Hagberg, Pieter Swart, and Daniel S Chult. Exploring network structure, dynamics, and function using networkx. Technical report, Los Alamos National Lab.(LANL), Los Alamos, NM (United States), 2008.
- William L. Hamilton, Zhitao Ying, and Jure Leskovec. Inductive representation learning on large graphs. In Isabelle Guyon, Ulrike von Luxburg, Samy Bengio, Hanna M. Wallach, Rob Fergus, S. V. N. Vishwanathan, and Roman Garnett (eds.), *Advances in Neural Information Processing Systems 30: Annual Conference on Neural Information Processing Systems 2017, December 4-9, 2017, Long Beach, CA, USA*, pp. 1024–1034, 2017. URL <https://proceedings.neurips.cc/paper/2017/hash/5dd9db5e033da9c6fb5ba83c7a7e9-Abstract.html>.
- Demis Hassabis. Using ai to accelerate scientific discovery, 2023. URL <https://www.nvidia.com/en-us/on-demand/session/gtcspring23-s51831/>.
- Kaiming He, Xinlei Chen, Saining Xie, Yanghao Li, Piotr Dollár, and Ross Girshick. Masked autoencoders are scalable vision learners. In *Proceedings of the IEEE/CVF conference on computer vision and pattern recognition*, pp. 16000–16009, 2022.
- Weihua Hu, Matthias Fey, Marinka Zitnik, Yuxiao Dong, Hongyu Ren, Bowen Liu, Michele Catasta, and Jure Leskovec. Open graph benchmark: Datasets for machine learning on graphs. *Advances in neural information processing systems*, 33:22118–22133, 2020.
- Weihua Hu, Matthias Fey, Hongyu Ren, Maho Nakata, Yuxiao Dong, and Jure Leskovec. Ogb-lsc: A large-scale challenge for machine learning on graphs. *arXiv preprint arXiv:2103.09430*, 2021.
- George Karypis and Vipin Kumar. Metis: A software package for partitioning unstructured graphs, partitioning meshes, and computing fill-reducing orderings of sparse matrices. Technical report, University of Minnesota Twin Cities, Department of Computer Science and Engineering, 1997.
- Jinwoo Kim, Dat Nguyen, Seonwoo Min, Sungjun Cho, Moontae Lee, Honglak Lee, and Seunghoon Hong. Pure transformers are powerful graph learners. *Advances in Neural Information Processing Systems*, 35:14582–14595, 2022.
- Thomas N. Kipf and Max Welling. Semi-supervised classification with graph convolutional networks. In *5th International Conference on Learning Representations, ICLR 2017, Toulon, France, April 24-26, 2017, Conference Track Proceedings*. OpenReview.net, 2017. URL <https://openreview.net/forum?id=SJU4ayYgl>.
- Alex Krizhevsky, Ilya Sutskever, and Geoffrey E Hinton. Imagenet classification with deep convolutional neural networks. In F. Pereira, C. J. C. Burges, L. Bottou, and K. Q. Weinberger (eds.), *Advances in Neural Information Processing Systems 25*, pp. 1097–1105. Curran Associates, Inc., 2012.
- Guohao Li, Chenxin Xiong, Ali K. Thabet, and Bernard Ghanem. Deepergcn: All you need to train deeper gcns. *CoRR*, abs/2006.07739, 2020. URL <https://arxiv.org/abs/2006.07739>.

-
- Guohao Li, Matthias Müller, Bernard Ghanem, and Vladlen Koltun. Training graph neural networks with 1000 layers. In Marina Meila and Tong Zhang (eds.), *Proceedings of the 38th International Conference on Machine Learning, ICML 2021, 18-24 July 2021, Virtual Event*, volume 139 of *Proceedings of Machine Learning Research*, pp. 6437–6449. PMLR, 2021. URL <http://proceedings.mlr.press/v139/li21o.html>.
- Ze Liu, Yutong Lin, Yue Cao, Han Hu, Yixuan Wei, Zheng Zhang, Stephen Lin, and Baining Guo. Swin transformer: Hierarchical vision transformer using shifted windows. In *2021 IEEE/CVF International Conference on Computer Vision, ICCV 2021, Montreal, QC, Canada, October 10-17, 2021*, pp. 9992–10002. IEEE, 2021. doi: 10.1109/ICCV48922.2021.00986. URL <https://doi.org/10.1109/ICCV48922.2021.00986>.
- Ilya Loshchilov and Frank Hutter. Decoupled weight decay regularization. *arXiv preprint arXiv:1711.05101*, 2017.
- Shengjie Luo, Tianlang Chen, Yixian Xu, Shuxin Zheng, Tie-Yan Liu, Liwei Wang, and Di He. One transformer can understand both 2d & 3d molecular data. In *International Conference on Learning Representations*, 2023.
- Kwan Mei-Ko. Graphic programming using odd or even points. *Chinese Math*, 1:237–277, 1962.
- Inc Midjourney. Midjourney, 2023. URL <https://www.midjourney.com>.
- Erxue Min, Runfa Chen, Yatao Bian, Tingyang Xu, Kangfei Zhao, Wenbing Huang, Peilin Zhao, Junzhou Huang, Sophia Ananiadou, and Yu Rong. Transformer for graphs: An overview from architecture perspective. *CoRR*, abs/2202.08455, 2022. URL <https://arxiv.org/abs/2202.08455>.
- Luis Müller, Mikhail Galkin, Christopher Morris, and Ladislav Rampásek. Attending to graph transformers. *arXiv preprint arXiv:2302.04181*, 2023.
- Maho Nakata and Tomomi Shimazaki. Pubchemqc project: A large-scale first-principles electronic structure database for data-driven chemistry. *J. Chem. Inf. Model.*, 57(6):1300–1308, 2017. doi: 10.1021/acs.jcim.7b00083. URL <https://doi.org/10.1021/acs.jcim.7b00083>.
- Open-AI. Chatgpt. <https://chat.openai.com/>, 2023.
- Long Ouyang, Jeffrey Wu, Xu Jiang, Diogo Almeida, Carroll Wainwright, Pamela Mishkin, Chong Zhang, Sandhini Agarwal, Katarina Slama, Alex Ray, et al. Training language models to follow instructions with human feedback. *Advances in Neural Information Processing Systems*, 35: 27730–27744, 2022.
- Luis Perez and Jason Wang. The effectiveness of data augmentation in image classification using deep learning. *arXiv preprint arXiv:1712.04621*, 2017.
- Alec Radford, Karthik Narasimhan, Tim Salimans, and Ilya Sutskever. Improving language understanding by generative pre-training, 2018.
- Alec Radford, Jeffrey Wu, Rewon Child, David Luan, Dario Amodei, Ilya Sutskever, et al. Language models are unsupervised multitask learners. *OpenAI blog*, 1(8):9, 2019.
- Colin Raffel, Noam Shazeer, Adam Roberts, Katherine Lee, Sharan Narang, Michael Matena, Yanqi Zhou, Wei Li, and Peter J Liu. Exploring the limits of transfer learning with a unified text-to-text transformer. *The Journal of Machine Learning Research*, 21(1):5485–5551, 2020.
- Ladislav Rampásek, Michael Galkin, Vijay Prakash Dwivedi, Anh Tuan Luu, Guy Wolf, and Dominique Beaini. Recipe for a general, powerful, scalable graph transformer. In *NeurIPS*, 2022. URL http://papers.nips.cc/paper_files/paper/2022/hash/5d4834a159f1547b267a05a4e2b7cf5e-Abstract-Conference.html.
- Jeff Rasley, Samyam Rajbhandari, Olatunji Ruwase, and Yuxiong He. Deepspeed: System optimizations enable training deep learning models with over 100 billion parameters. In *Proceedings of the 26th ACM SIGKDD International Conference on Knowledge Discovery & Data Mining*, pp. 3505–3506, 2020.

-
- T. Konstantin Rusch, Michael M. Bronstein, and Siddhartha Mishra. A survey on oversmoothing in graph neural networks, 2023.
- Christoph Schuhmann, Romain Beaumont, Richard Vencu, Cade Gordon, Ross Wightman, Mehdi Cherti, Theo Coombes, Aarush Katta, Clayton Mullis, Mitchell Wortsman, Patrick Schramowski, Srivatsa Kundurthy, Katherine Crowson, Ludwig Schmidt, Robert Kaczmarczyk, and Jenia Jitsev. LAION-5B: an open large-scale dataset for training next generation image-text models. In *NeurIPS*, 2022. URL http://papers.nips.cc/paper_files/paper/2022/hash/a1859debfb3b59d094f3504d5ebb6c25-Abstract-Datasets_and_Benchmarks.html.
- Rico Sennrich, Barry Haddow, and Alexandra Birch. Neural machine translation of rare words with subword units. In *Proceedings of the 54th Annual Meeting of the Association for Computational Linguistics, ACL 2016, August 7-12, 2016, Berlin, Germany, Volume 1: Long Papers*. The Association for Computer Linguistics, 2016. doi: 10.18653/v1/p16-1162. URL <https://doi.org/10.18653/v1/p16-1162>.
- Yunsheng Shi, Zhengjie Huang, Shikun Feng, Hui Zhong, Wenjin Wang, and Yu Sun. Masked label prediction: Unified message passing model for semi-supervised classification. *arXiv preprint arXiv:2009.03509*, 2020.
- Mohammad Shoeybi, Mostofa Patwary, Raul Puri, Patrick LeGresley, Jared Casper, and Bryan Catanzaro. Megatron-lm: Training multi-billion parameter language models using model parallelism. *CoRR*, abs/1909.08053, 2019. URL <http://arxiv.org/abs/1909.08053>.
- Chuxiong Sun, Jie Hu, Hongming Gu, Jinpeng Chen, and Mingchuan Yang. Adaptive graph diffusion networks. *arXiv preprint arXiv:2012.15024*, 2020.
- Damian Szklarczyk, Annika L Gable, David Lyon, Alexander Junge, Stefan Wyder, Jaime Huerta-Cepas, Milan Simonovic, Nadezhda T Doncheva, John H Morris, Peer Bork, et al. String v11: protein-protein association networks with increased coverage, supporting functional discovery in genome-wide experimental datasets. *Nucleic acids research*, 47(D1):D607–D613, 2019.
- Hugo Touvron, Thibaut Lavril, Gautier Izacard, Xavier Martinet, Marie-Anne Lachaux, Timothée Lacroix, Baptiste Rozière, Naman Goyal, Eric Hambro, Faisal Azhar, et al. Llama: Open and efficient foundation language models. *arXiv preprint arXiv:2302.13971*, 2023.
- Ashish Vaswani, Noam Shazeer, Niki Parmar, Jakob Uszkoreit, Llion Jones, Aidan N Gomez, Łukasz Kaiser, and Illia Polosukhin. Attention is all you need. In *Advances in Neural Information Processing Systems*, pp. 5998–6008, 2017.
- Alex Wang, Yada Pruksachatkun, Nikita Nangia, Amanpreet Singh, Julian Michael, Felix Hill, Omer Levy, and Samuel R. Bowman. Superglue: A stickier benchmark for general-purpose language understanding systems. In Hanna M. Wallach, Hugo Larochelle, Alina Beygelzimer, Florence d’Alché-Buc, Emily B. Fox, and Roman Garnett (eds.), *Advances in Neural Information Processing Systems 32: Annual Conference on Neural Information Processing Systems 2019, NeurIPS 2019, December 8-14, 2019, Vancouver, BC, Canada*, pp. 3261–3275, 2019a. URL <https://proceedings.neurips.cc/paper/2019/hash/4496bf24afe7fab6f046bf4923da8de6-Abstract.html>.
- Alex Wang, Amanpreet Singh, Julian Michael, Felix Hill, Omer Levy, and Samuel R. Bowman. GLUE: A multi-task benchmark and analysis platform for natural language understanding. In *7th International Conference on Learning Representations, ICLR 2019, New Orleans, LA, USA, May 6-9, 2019*. OpenReview.net, 2019b. URL <https://openreview.net/forum?id=rJ4km2R5t7>.
- Jason Wei, Maarten Bosma, Vincent Y Zhao, Kelvin Guu, Adams Wei Yu, Brian Lester, Nan Du, Andrew M Dai, and Quoc V Le. Finetuned language models are zero-shot learners. *arXiv preprint arXiv:2109.01652*, 2021.
- Douglas Brent West et al. *Introduction to graph theory*, volume 2. Prentice hall Upper Saddle River, 2001.

Thomas Wolf, Lysandre Debut, Victor Sanh, Julien Chaumond, Clement Delangue, Anthony Moi, Pierric Cistac, Tim Rault, Rémi Louf, Morgan Funtowicz, Joe Davison, Sam Shleifer, Patrick von Platen, Clara Ma, Yacine Jernite, Julien Plu, Canwen Xu, Teven Le Scao, Sylvain Gugger, Mariama Drame, Quentin Lhoest, and Alexander M. Rush. Transformers: State-of-the-art natural language processing. In *Proceedings of the 2020 Conference on Empirical Methods in Natural Language Processing: System Demonstrations*, pp. 38–45, Online, October 2020. Association for Computational Linguistics. URL <https://www.aclweb.org/anthology/2020.emnlp-demos.6>.

Zhenqin Wu, Bharath Ramsundar, Evan N. Feinberg, Joseph Gomes, Caleb Geniesse, Aneesh S. Pappu, Karl Leswing, and Vijay S. Pande. Moleculenet: A benchmark for molecular machine learning. *CoRR*, abs/1703.00564, 2017. URL <http://arxiv.org/abs/1703.00564>.

Zonghan Wu, Shirui Pan, Fengwen Chen, Guodong Long, Chengqi Zhang, and S Yu Philip. A comprehensive survey on graph neural networks. *IEEE transactions on neural networks and learning systems*, 32(1):4–24, 2020.

Keyulu Xu, Weihua Hu, Jure Leskovec, and Stefanie Jegelka. How powerful are graph neural networks? In *7th International Conference on Learning Representations, ICLR 2019, New Orleans, LA, USA, May 6-9, 2019*. OpenReview.net, 2019. URL <https://openreview.net/forum?id=ryGs6iA5Km>.

Chengxuan Ying, Tianle Cai, Shengjie Luo, Shuxin Zheng, Guolin Ke, Di He, Yanming Shen, and Tie-Yan Liu. Do transformers really perform badly for graph representation? *Advances in Neural Information Processing Systems*, 34:28877–28888, 2021.

Jason Yosinski, Jeff Clune, Yoshua Bengio, and Hod Lipson. How transferable are features in deep neural networks? *Advances in neural information processing systems*, 27, 2014.

Hanqing Zeng, Muhan Zhang, Yinglong Xia, Ajitesh Srivastava, Andrey Malevich, Rajgopal Kannan, Viktor Prasanna, Long Jin, and Ren Chen. Decoupling the depth and scope of graph neural networks. *Advances in Neural Information Processing Systems*, 34:19665–19679, 2021.

Muhan Zhang and Yixin Chen. Link prediction based on graph neural networks. In Samy Bengio, Hanna M. Wallach, Hugo Larochelle, Kristen Grauman, Nicolò Cesa-Bianchi, and Roman Garnett (eds.), *Advances in Neural Information Processing Systems 31: Annual Conference on Neural Information Processing Systems 2018, NeurIPS 2018, December 3-8, 2018, Montréal, Canada*, pp. 5171–5181, 2018. URL <https://proceedings.neurips.cc/paper/2018/hash/53f0d7c537d99b3824f0f99d62ea2428-Abstract.html>.

A DATASETS

The detailed statistics of datasets are reported in Tab. 8.

Table 8: Statistics of graph-/edge-/node-level datasets. Here ‘BC’ stands for binary classification.

datasets	# of graphs	avg # of nodes	avg # of edges	task-type	metrics
ogbg-molpcba	437,929	26.0	28.1	BC	AP
PCQM4Mv2	3,746,619	14.14	14.56	regression	MAE
ogbl-ppa	1	576,289	30,326,273	multi-label BC	HR@100
ogbn-proteins	1	132,534	39,561,252	BC	ROC-AUC

A.1 SUBGRAPH SAMPLING

The subgraph sampling for different datasets of big graphs are shown in Tab. 9.

Table 9: Details of subgraph sampling for ogbl-ppa and ogbn-proteins datasets. ‘ctx’ means the context window. edge-ego means sampling subgraph around the central edge, and node-ego means around the central node.

dataset	sampling	depth	# neighbors	ctx
ogbl-ppa	edge-ego	1	14	256
ogbn-proteins	node-ego	9	1	256
		16	1	512
		24	1	1024
		42	1	2048

B MODELS

We list the model specifics in Tab. 10.

Table 10: Statistics of GraphGPT models of different sizes. The GraphGPT-base is of the same scale as Bert-base (Devlin et al., 2019).

model-size	hidden-size	# of layers	# of heads
mini	256	4	4
small	512	4	8
medium	512	8	8
base	768	12	12
large	1024	24	16

C IMPLEMENTATION DETAILS

C.1 GRAPHS TO SEQUENCES OF TOKENS

The code is implemented with Pytorch. We use torch-geometric (Fey & Lenssen, 2019) to preprocess graphs, *e.g.*, subgraph sampling and etc. We use Networkx (Hagberg et al., 2008) to Eulerize the (sub)graphs if needed and then find the (semi-)Eulerian paths. We write our own tokenizer to convert the (semi-)Eulerian paths to sequences of tokens. The token vocabulary is built for each dataset separately.

C.2 MODEL BACKBONE

We adopt Llama’s transformer decoder (Touvron et al., 2023) implemented in the Hugging Face’s transformers package (Wolf et al., 2020) as our backbone. We do not used Llama’s pre-trained weights. Instead, we train models of different scales as in Tab. 10 with random parameters initialization.

C.3 TRAINING

The models are pre-trained and fine-tuned on GPU clusters of V100-32G using DeepSpeed’s stage-2 schema with mixed precision (Rasley et al., 2020). Following the optimizer setting in Llama, we use AdamW (Loshchilov & Hutter, 2017) with the hyper-parameters $\beta_1 = 0.9$, $\beta_2 = 0.95$ and weight decay of 0.1 and gradient clipping of 1.0. We use a linear decay learning rate schedule with 1,000 warmup for pre-training only. The maximal learning rate in is 3×10^{-4} for pre-training and 3×10^{-5} for fine-tuning. To make full use of computing power, we pack several graph sequences together into one entry to maximize the context window (Raffel et al., 2020).

C.4 VOCABULARY

In NLP, the vocabulary is usually built by tokenizing the text data with the byte-pair encoding (BPE) algorithm (Sennrich et al., 2016). The resulting unique tokens form the vocabulary, and they are usually frequent subwords in the text corpus.

In our GraphGPT, the vocabulary is constructed very differently. We split the vocabulary into two parts, the first part contains the structural and special tokens, and they are dataset agnostic. The second part consists of the tokens that encode the semantics information of the dataset, such as node and edge attributes.

App. E shows an example. In the graph sequence, tokens ‘1’, ‘2’ and so on are structural tokens. ‘ogbl-ppa#node#0#17’ and ‘ogbl-ppa#node#1#1959’ are semantics tokens. <gsum> and <eos> in Fig. 1 are special tokens.

D GRAPH-LEVEL TASK

D.1 GRAPHS TO SEQUENCES OF TOKENS

Below is one example of 2D molecular graphs in the ogbg-molpcba dataset in torch-geometric data format (Fey & Lenssen, 2019).

```
Data(x=[4, 9], edge_index=[2, 6], edge_attr=[6, 3], y=[128])
```

The graph has 4 nodes and 3 edges. The source and destination nodes of the edges are recorded in ‘edge_index’, and its dimension is $(2, 2 \cdot \text{number_of_nodes})$ for undirected graphs. ‘x’ is the node attributes of 9 dimensions, and ‘edge_attr’ stores the edge attributes of 3 dimensions.

The node and edge attributes of the graphs are numbers. If we directly discretize them into tokens, i.e., using one token to represent each unique number, the numbers that appear few times in the dataset cannot be well-trained. At the same time, the vocabulary may blow up. Therefore, we split them into single digits and represent them with the combination of the following tokens. They are dataset agnostic, and can be shared across different datasets.

<->, <.>, <0>, <1>, <2>, <3>, <4>, <5>, <6>, <7>, <8>, <9>

The resulting vocabulary is 556 for both ogbg-molpcba and PCQM4Mv2.

Below shows the tokens from one of the possible (semi-)Eulerian paths of the above molecular graph.

```
[ '1', 'ogbg-molpcba#node#0#1', '<7>', 'ogbg-molpcba#node#2#1',  
  '<1>', 'ogbg-molpcba#node#3#1', '<5>', 'ogbg-molpcba#node#6#1',  
  '<1>', 'ogbg-molpcba#edge#0#1', '<1>', '2', '3', 'ogbg-molpcba#node#0#1',  
  '<5>', 'ogbg-molpcba#node#2#1', '<4>', 'ogbg-molpcba#node#3#1',  
  '<5>', 'ogbg-molpcba#node#4#1', '<3>', 'ogbg-molpcba#node#6#1',  
  '<2>', '2', 'ogbg-molpcba#node#0#1', '<5>', 'ogbg-molpcba#node#2#1',  
  '<3>', 'ogbg-molpcba#node#3#1', '<5>', 'ogbg-molpcba#node#6#1', '<1>', '4',  
  'ogbg-molpcba#node#0#1', '<5>', 'ogbg-molpcba#node#2#1', '<4>',  
  'ogbg-molpcba#node#3#1', '<5>', 'ogbg-molpcba#node#4#1', '<3>',  
  'ogbg-molpcba#node#6#1', '<2>' ]
```

In the sequence of tokens above, for the node ‘1’, we can deduce that its 9 dimensional attributes are $(7, 0, 1, 5, 0, 0, 1, 0, 0)$. Node ‘1’ is connected to ‘2’ with edge attributes $(1, 0, 0)$. We set 0 as the default value of the attributes in this dataset, and do not encode it into tokens.

In the (semi-)Eulerian path, a node may appear several times. We append its attributes tokens to one of its appearances randomly. This can prevent the model from copying the attributes from the previous appearance, and also shorten the resulting sequence.

For a graph obtained from Eulerization, an edge may present several times in the path. We apply the same logic to insert the edge attributes tokens.

As in the above sequence, node '2' appears two times, and its node attributes tokens are appended after its second appearance. There is no tokens encode the edge attributes of edge between '2' and '3', which implies the edge attributes are default value (0, 0, 0).

In the ablation study on node re-index in Sec. 3.5.2, the resulting tokens without node re-indexing of the same example above is shown below. Without re-indexing, the starting node will keep its original notation, which is '4' in this case.

```
[ '4', 'ogbg-molpcba#node#0#1', '<7>', 'ogbg-molpcba#node#2#1',
  '<1>', 'ogbg-molpcba#node#3#1', '<5>', 'ogbg-molpcba#node#6#1',
  '<1>', 'ogbg-molpcba#edge#0#1', '<1>', '2', '1', 'ogbg-molpcba#node#0#1',
  '<5>', 'ogbg-molpcba#node#2#1', '<4>', 'ogbg-molpcba#node#3#1',
  '<5>', 'ogbg-molpcba#node#4#1', '<3>', 'ogbg-molpcba#node#6#1',
  '<2>', '2', 'ogbg-molpcba#node#0#1', '<5>', 'ogbg-molpcba#node#2#1',
  '<3>', 'ogbg-molpcba#node#3#1', '<5>', 'ogbg-molpcba#node#6#1', '<1>',
  '3', 'ogbg-molpcba#node#0#1', '<5>', 'ogbg-molpcba#node#2#1', '<4>',
  'ogbg-molpcba#node#3#1', '<5>', 'ogbg-molpcba#node#4#1', '<3>',
  'ogbg-molpcba#node#6#1', '<2>' ]
```

D.2 MODEL, PRE-TRAINING AND FINE-TUNING

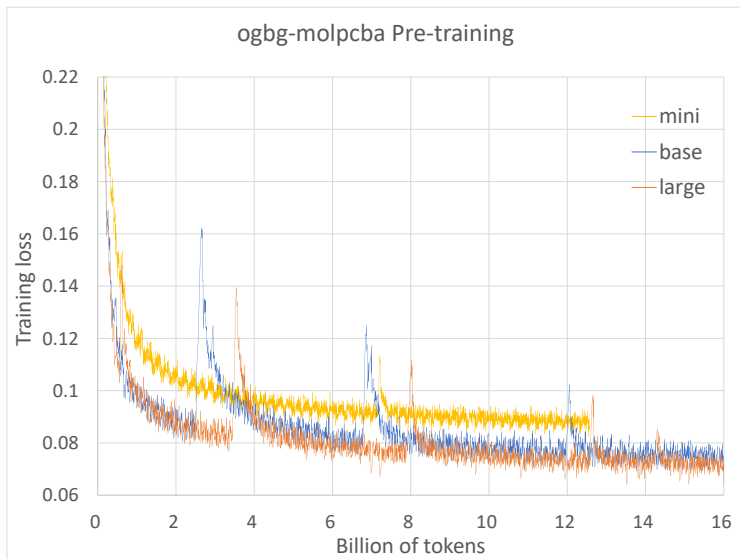


Figure 2: Training loss versus tokens of ogbg-molpcba dataset for models small/base/large as in Tab. 10. They are all trained on 12.6 B to 16 B tokens with a batch size of 0.4M tokens.

We set the context window to be 1024 so that the token sequence of all the molecules can be fit in. We use the mini-batch of 1024 and 1920 sequences for the ogbg-molpcba and PYQM4Mv2 datasets respectively. The total update-step is 4.3×10^4 and 1.8×10^6 .

E EDGE-LEVEL TASK

E.1 GRAPHS TO SEQUENCES OF TOKENS

The whole ogbl-ppa dataset is summarized in torch-geometric format as follows.

```
Data(num_nodes=576289, edge_index=[2, 42463862], x=[576289, 58])
```

It has 576289 nodes and 21231931 edges in the training data. 'x' is the one-hot representation of the species that the node (protein) belongs to.

We sample a subgraph from it as below.

```
Data(num_nodes=30, root_n_id=[2], edge_index=[2, 84], x=[30, 2])
```

It has 30 nodes, 42 edges as in 'edge_index'. 'x' is the node attributes of 2 dimensions, and it encodes the node identity as described in Sec. 2.2.3. We partition the nodes (proteins) based on the associated species. The number of proteins inside each species varies from 616 to 41017. Finally we use 58 tokens for species and 41017 tokens for the local indices. Combined with the tokens for the structure and the special tokens, the total vocabulary is 41231.

Here 'root_n_id' records the two seed nodes, and the subgraph is sampled centered around them. The resulting tokens from one of the possible (semi-)Eulerian paths are:

```
['1', '2', '3', 'ogbl-ppa#node#0#17', 'ogbl-ppa#node#1#1959', '4', '5', 'ogbl-ppa#node#0#17', 'ogbl-ppa#node#1#2460', '6', '7', 'ogbl-ppa#node#0#17', 'ogbl-ppa#node#1#3566', '6', '8', 'ogbl-ppa#node#0#17', 'ogbl-ppa#node#1#4145', '6', '9', 'ogbl-ppa#node#0#20', 'ogbl-ppa#node#1#5334', '10', 'ogbl-ppa#node#0#27', 'ogbl-ppa#node#1#17324', '6', 'ogbl-ppa#node#0#17', 'ogbl-ppa#node#1#6850', '11', 'ogbl-ppa#node#0#17', 'ogbl-ppa#node#1#5498', '6', '12', 'ogbl-ppa#node#0#17', 'ogbl-ppa#node#1#5776', '6', '4', 'ogbl-ppa#node#0#17', 'ogbl-ppa#node#1#8183', '2', '5', '2', '13', 'ogbl-ppa#node#0#17', 'ogbl-ppa#node#1#3514', '2', 'ogbl-ppa#node#0#17', 'ogbl-ppa#node#1#9374', '14', 'ogbl-ppa#node#0#17', 'ogbl-ppa#node#1#6164', '15', 'ogbl-ppa#node#0#17', 'ogbl-ppa#node#1#8368', '2', '6', '16', 'ogbl-ppa#node#0#17', 'ogbl-ppa#node#1#10803', '6', '17', 'ogbl-ppa#node#0#17', 'ogbl-ppa#node#1#11465', '6', '10', '18', 'ogbl-ppa#node#0#20', 'ogbl-ppa#node#1#16505', '6', '19', 'ogbl-ppa#node#0#17', 'ogbl-ppa#node#1#15071', '2', '20', 'ogbl-ppa#node#0#17', 'ogbl-ppa#node#1#7761', '2', '21', 'ogbl-ppa#node#0#17', 'ogbl-ppa#node#1#8828', '2', '22', 'ogbl-ppa#node#0#17', 'ogbl-ppa#node#1#14477', '2', '23', 'ogbl-ppa#node#0#17', 'ogbl-ppa#node#1#16026', '2', '24', 'ogbl-ppa#node#0#17', 'ogbl-ppa#node#1#16825', '6', '25', 'ogbl-ppa#node#0#17', 'ogbl-ppa#node#1#17615', '19', '25', '2', '26', 'ogbl-ppa#node#0#17', 'ogbl-ppa#node#1#19524', '2', '27', 'ogbl-ppa#node#0#17', 'ogbl-ppa#node#1#17854', '6', '28', 'ogbl-ppa#node#0#17', 'ogbl-ppa#node#1#17733', '6', '29', 'ogbl-ppa#node#0#27', 'ogbl-ppa#node#1#23255', '6', '30', 'ogbl-ppa#node#0#17', 'ogbl-ppa#node#1#19700', '6', '27', '1', 'ogbl-ppa#node#0#17', 'ogbl-ppa#node#1#20474']
```

In the ablation study on node identity encoding in Sec. 3.5.3, an example of the subgraph sampled from ogbl-ppa without identity encoding is shown below.

```
Data(num_nodes=30, root_n_id=[2], edge_index=[2, 136], x=[30, 1])
```

Different from the subgraph with node identity encoded in 'x', its node attribute 'x' contains only the information of the node's (protein) hosting species. It cannot be used to uniquely identify the nodes. The vocabulary decreases from 41231 to 214.

The resulting tokens from one of its possible (semi-)Eulerian paths is below.

```
['1', '2', '3', '4', 'ogbl-ppa#node#0#17', '5', '6', '7', '5', '8', '9', '1', 'ogbl-ppa#node#0#17', '10', 'ogbl-ppa#node#0#17', '11', 'ogbl-ppa#node#0#17', '3', 'ogbl-ppa#node#0#17', '11', '12', '1', '5', '13', 'ogbl-ppa#node#0#17', '5', '14', 'ogbl-ppa#node#0#17', '5', '9', '10', '8', 'ogbl-ppa#node#0#17']
```

```

#0#17', '3', '15', 'ogbl-ppa#node#0#17', '3', '16', 'ogbl-ppa#
node#0#17', '3', '2', 'ogbl-ppa#node#0#20', '17', 'ogbl-ppa#
node#0#27', '1', '18', 'ogbl-ppa#node#0#20', '1', '19', 'ogbl-
ppa#node#0#17', '3', '9', 'ogbl-ppa#node#0#17', '20', 'ogbl-
ppa#node#0#17', '10', '3', '21', '3', '5', '10', '12', 'ogbl-
ppa#node#0#17', '3', '22', 'ogbl-ppa#node#0#17', '3', '17',
'18', '3', '23', '13', '24', '5', '25', 'ogbl-ppa#node#0#17',
'23', 'ogbl-ppa#node#0#17', '21', 'ogbl-ppa#node#0#17', '20',
'5', '26', 'ogbl-ppa#node#0#17', '5', '22', '24', 'ogbl-ppa#
node#0#17', '23', '5', '27', '6', 'ogbl-ppa#node#0#17', '28',
'ogbl-ppa#node#0#17', '7', 'ogbl-ppa#node#0#17', '28', '5',
'ogbl-ppa#node#0#17', '27', 'ogbl-ppa#node#0#17', '29', 'ogbl-
ppa#node#0#17', '5', '30', 'ogbl-ppa#node#0#17', '5', '19',
'5', '12', '20', '1']

```

E.2 MODEL, PRE-TRAINING AND FINE-TUNING

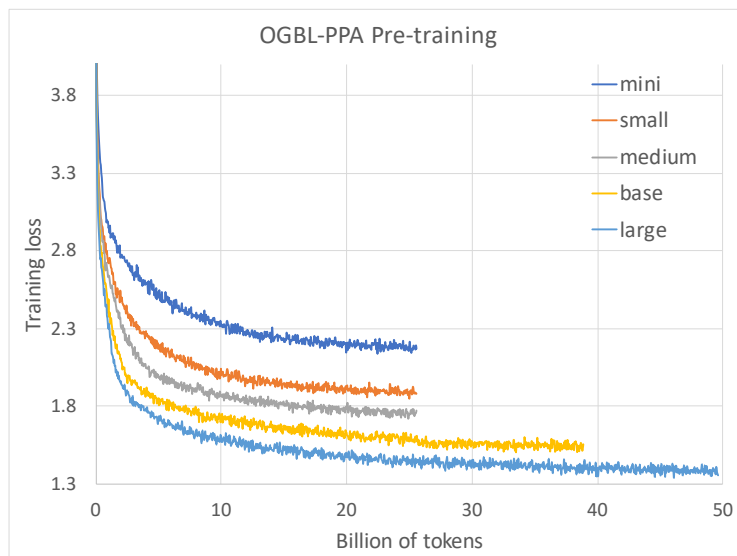


Figure 3: Training loss versus tokens of ogbl-ppa dataset for models mini/small/medium/base/large as in Tab. 10. They are all trained on 25.6 B tokens with a batch size of 0.4M (*i.e.*, 1600×256) tokens. GraphGPT-base and GraphGPT-large are further trained with additional tokens to attain better fine-tuning performance.

In pre-training stage, we use the mini-batch of 1600 sequences of 256 tokens. The total update-step is 6.25×10^4 . In fine-tuning stage, we use the mini-batch of 4096 sequences of maximal 256 tokens.

The pre-training loss versus the number of tokens is shown in Fig. 3. In general, larger model results in lower pre-training loss, and better results in down-stream fine-tuning tasks. The fine-tuning results of link prediction is shown in Tab. 11. Pre-training can improve the downstream task substantially (see Fig. 4).

E.3 NODE IDENTITY ENCODING

The comparison between models trained with and without node identity encoding is shown in Fig. 5. The node identity encoding can achieve much better results.

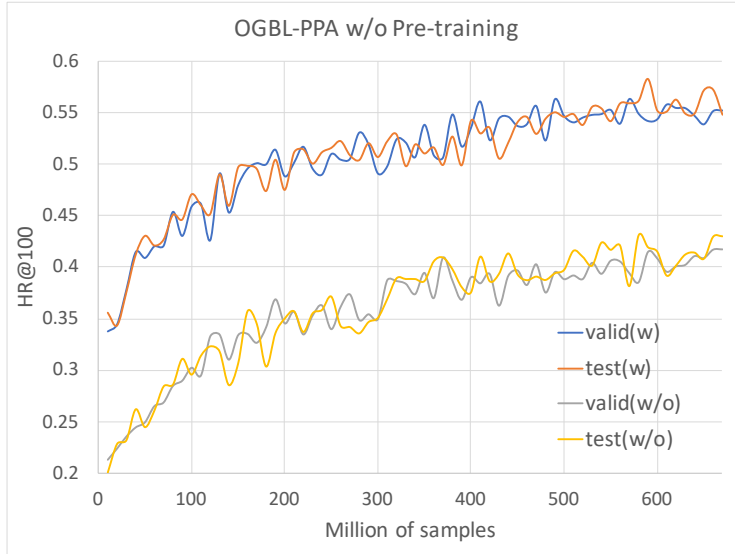


Figure 4: The ablation study of pre-training for ogbl-ppa. Evaluation metric HR@100 on the valid/test data versus the number of samples fine-tuned. ‘w’ and ‘w/o’ indicate whether pre-training is employed or not. ‘w’ means the model is pre-trained with 25.6 B tokens first, and then fine-tuned with the link prediction task. ‘w/o’ indicates that the model is trained with the supervised link prediction task directly with random parameters initialization. We use GraphGPT-mini to save time and computing resources.

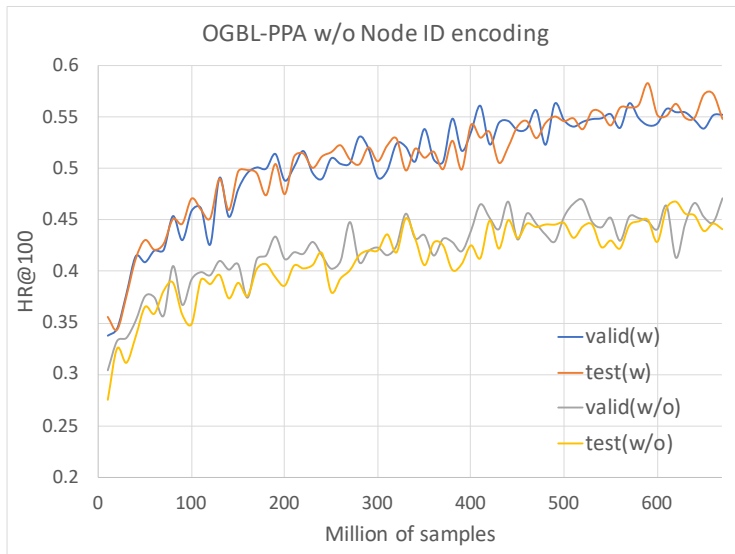


Figure 5: The ablation study of node identity encoding for ogbl-ppa. Evaluation metric HR@100 on the valid/test data versus the number of samples fine-tuned. ‘w’ and ‘w/o’ indicate whether the node is encoded with two tokens uniquely or not. Both ‘w’ and ‘w/o’ are pre-trained with 25.6 B tokens first, and then fine-tuned with the link prediction task. After fine-tuning with about 500 M samples, the results become stable. The model is GraphGPT-mini.

Table 11: Edge-level link prediction task results of the ogbl-ppa dataset of different model size.

Models		HR@100 (%)		Params
		Test	Valid	
GraphGPT	mini (w/o pre-training)	41.28±1.35	40.14±1.01	14.75M
	mini	55.56±1.14	54.87±0.66	14.75M
	small	57.25±1.34	58.78±0.68	37.89M
	medium	60.08±1.18	61.01±0.77	54.67M
	base	64.98±1.73	66.68±1.33	144.93M
	large	67.15±1.36	68.60±1.40	444.92M

E.4 OTHER DATASETS

We also conduct the experiment on a small dataset ogbl-ddi. The performance is not good. It either implies that we need more experiments to find suitable hyper-parameters, or indicates that GraphGPT might not be a good choice for small dense graphs. ogbl-ddi has around 14.67% edges of the corresponding complete graph. In contrast, ogbl-ppa has only 0.018% edges of the complete graph.

F NODE-LEVEL TASK

F.1 GRAPHS TO SEQUENCES OF TOKENS

The entire ogbn-proteins dataset is a large graph as follows.

```
Data(num_nodes=132534, edge_index=[2, 79122504], edge_attr
      =[79122504, 8], node_species=[132534, 1], y=[132534, 112])
```

It has 132,534 nodes and 39,561,252 edges. ‘node_species’ stores the species’ numeric id that the node (proteins) belongs to.

One sampled subgraph in the torch-geometric data format is:

```
Data(num_nodes=10, root_n_id=0, edge_index=[2, 22], edge_attr=[22,
      8], y=[10, 112], x=[10, 2])
```

It has 10 nodes, 11 edges as in ‘edge_index’. Edge attributes is stored in ‘edge_attr’ of dimension 8. ‘x’ is the node attributes of 2 dimensions, and it encodes the node identity as described in Sec. 2.2.3. Its first dimension (token) represents the species, and the second is local numbering of each protein inside its species. Similar to the ogbl-ppa dataset, the identity encoding of 132,534 nodes occupies 25,465 tokens in the vocabulary, and the total vocabulary is 25,620.

‘y’ records the labels for the supervised node-level task. ‘root_n_id’ represents the target node, and the subgraph is sampled centered around it.

The resulting tokens from one of the possible (semi-)Eulerian paths are as follows.

```
[ '1', 'ogbn-proteins#node#0#3702', 'ogbn-proteins#node#1#16267', '
ogbn-proteins#edge#7#1', '<1>', '<6>', '<4>', '2', 'ogbn-
proteins#node#0#3702', 'ogbn-proteins#node#1#6896', 'ogbn-
proteins#edge#4#1', '<3>', '<4>', '<0>', '3', 'ogbn-proteins#
node#0#3702', 'ogbn-proteins#node#1#4121', 'ogbn-proteins#edge
#4#1', '<3>', '<9>', '<8>', '4', 'ogbn-proteins#node#0#3702',
'ogbn-proteins#node#1#3963', 'ogbn-proteins#edge#4#1', '<1>',
'<5>', '<3>', '5', 'ogbn-proteins#node#0#3702', 'ogbn-proteins
#node#1#8259', 'ogbn-proteins#edge#4#1', '<4>', '<8>', 'ogbn-
proteins#edge#7#1', '<2>', '<1>', '<5>', '6', '7', 'ogbn-
proteins#edge#7#1', '<4>', '<1>', '<8>', '8', 'ogbn-proteins#
node#0#3702', 'ogbn-proteins#node#1#1', '7', 'ogbn-proteins#
```

```

node#0#3702', 'ogbn-proteins#node#1#89', 'ogbn-proteins#edge
#7#1', '<3>', '<2>', '<1>', '6', 'ogbn-proteins#node#0#3702',
'ogbn-proteins#node#1#955', 'ogbn-proteins#edge#7#1', '<2>',
'<7>', '<0>', '9', 'ogbn-proteins#node#0#3702', 'ogbn-proteins
#node#1#7055', 'ogbn-proteins#edge#4#1', '<1>', '<6>', '<5>',
'10', 'ogbn-proteins#node#0#3702', 'ogbn-proteins#node
#1#10010', 'ogbn-proteins#edge#4#1', '<1>', '<6>', '<9>', '4',
'5', 'ogbn-proteins#edge#4#1', '<2>', '<0>', '<7>', '3']

```

The original edge attributes are 8-dimensional vector of 3 decimal numbers from 0.001 to 1. We split them into single digits and represent them with the combination of the digits tokens as in App. D.

To reduce the number of tokens in the resultant sequences further, we multiply the number with 1000 and then minus it by 1. So we do not need to encode ‘.’ any more. At the same time, we treat the value 0.001 (0 after the above transformation) as the default value and do not encode it with tokens.

F.2 MODEL, PRE-TRAINING AND FINE-TUNING

In the pre-training, we use the mini-batch of 2048 sequences of 256 tokens. The total update-step is 9.76×10^4 . In the fine-tuning, we use the mini-batch of 128 sequences of maximal 256 tokens.

The pre-training loss versus the number of tokens for various model sizes is shown in Fig. 6. In general, larger model results in lower training loss, and better results in down-stream fine-tuning tasks as in Tab. 12.

The loss of mini/small/medium models are almost saturated after training with 25.6 B tokens. In contrast, base/large models can be further pre-trained as the loss keeps decreasing.

Fig. 8 shows that pre-training can improve the results significantly.

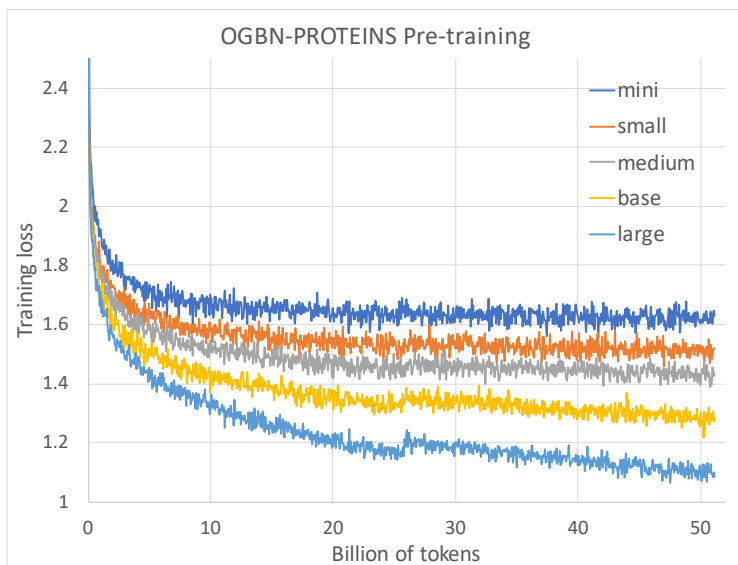


Figure 6: Pre-training loss versus tokens of ogbn-proteins dataset for models mini/small/medium/base/large as in Tab. 10. They are all trained on 51.2 B tokens with a batch size of 0.52M (*i.e.*, 2048×256) tokens. The first 25.6 B tokens are trained with the maximal learning rate 3×10^{-4} , and the second 25.6 B tokens are trained with the maximal learning rate 1×10^{-4} . The learning rate scheduler is linear decay with 1000 warm-up steps.

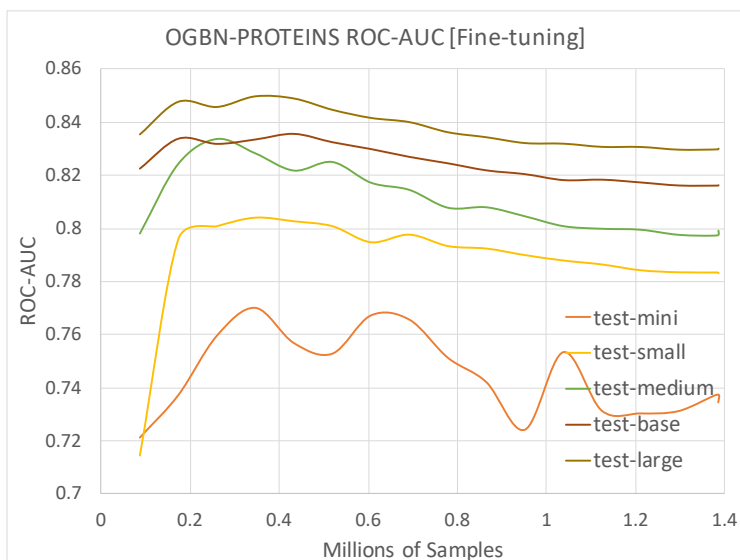


Figure 7: ROC-AUC metric on test data in the fine-tuning stage. x -axis is the number of samples trained during fine-tuning.

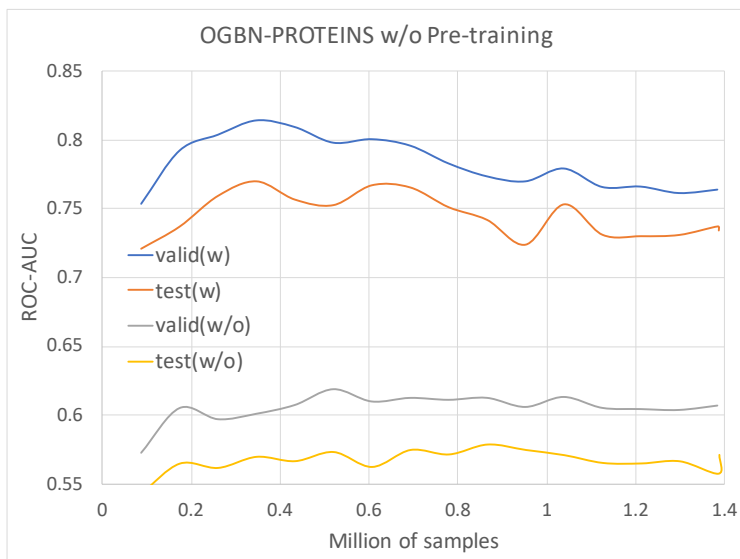


Figure 8: The ablation study of pre-training for ogbn-proteins of GraphGPT-mini. Evaluation metric ROC-AUC on the valid/test data versus the number of samples fine-tuned. 'w' and 'w/o' indicate whether pre-training is employed or not. 'w' means the model is pre-trained with 51.2 B tokens first, and then fine-tuned with the link prediction task. 'w/o' indicates that the model is trained with the supervised link prediction task directly with random parameters initialization. We use GraphGPT-mini to save time and computing resources.

Table 12: Node-level binary classification task results of ogbn-proteins dataset. The batch-size is 128, and the learning rate is 3×10^{-5} .

Models	ROC-AUC (%)		Params
	Test	Valid	
GraphGPT-mini (w/o pre-training)	57.52±0.36	61.19±0.08	10.76M
GraphGPT-mini	75.61±1.37	80.47±0.94	10.76M
GraphGPT-small	80.10±0.35	83.36±0.40	29.90M
GraphGPT-medium	82.71±0.52	86.18±0.28	46.68M
GraphGPT-base	83.37±0.15	87.68±0.25	132.94M
GraphGPT-large	84.80±0.18	89.35±0.24	428.94M

F.3 NODE IDENTITY ENCODING

The comparison between models trained with and without node identity encoding is shown in Fig. 9. The node identity encoding improves results.

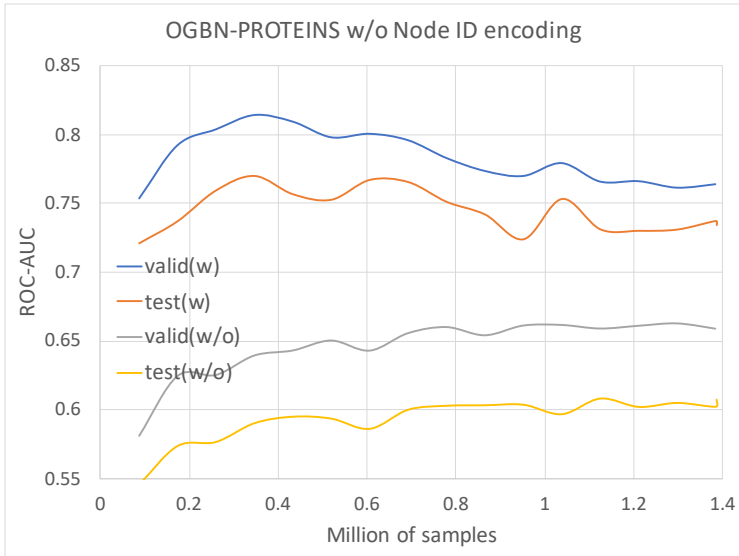


Figure 9: The ablation study of node identity encoding for ogbn-proteins of GraphGPT-mini. Evaluation metric ROC-AUC on the valid/test data versus the number of samples fine-tuned. ‘w’ and ‘w/o’ indicate whether the node is encoded with two tokens uniquely or not. Both ‘w’ and ‘w/o’ are pre-trained with 25.6 B tokens first, and then fine-tuned with the link prediction task. After fine-tuning with about 0.2 to 0.4 M samples, the results become stable for the model with node identity encoding.

G DISCUSSION ON LIMITATIONS

We discuss some limitations of GraphGPT for a comprehensive understanding the novel model.

Transferability. Due to the lack of shared semantics among different graph datasets, GraphGPT has to be pre-trained on target dataset itself and then fine-tuned. This may restrict its applicability in various graph tasks. However, there are two exceptions.

a). Structure-understanding GraphGPT. Graph structures are shared across all the graph datasets, for example, node degrees, motifs, edge directions and etc. We can pre-train a structure-understanding GraphGPT using structure information only, *i.e.*, removing all the semantics (node/edge attributes) in the graphs. This GraphGPT would be able to do any graph structure understanding related tasks,

if trained with enough data and large model size. Besides, it could be further pre-trained later on specific datasets with semantics information.

b). Domain specific GraphGPT. For example, molecular datasets share the same semantics information, *i.e.*, nodes (atoms) and edges (bonds). We can collect all available molecular datasets and pre-train a molecule-understanding GraphGPT. It can then be fine-tuned on various molecule datasets, and would have a wide application in drug and material research.

Dataset size. When the graph datasets for pre-train and fine-tune are small or medium, GraphGPT might not perform well, for example, ogbn-proteins and ogbg-molpcba datasets. It could be overcome by collecting more data of the same semantics for pre-training/fine-tuning. In addition, utilizing the above mentioned ‘structure-understanding GraphGPT’ and further pre-training on the dataset with semantics could also be helpful.

Compute budget. The pre-training on one big graph (ogbn-proteins and ogbl-ppa) and many small graphs (PCQM4M-v2) with large model sizes (50M+ parameters) are very computationally expensive.

For example, pre-training a GraphGPT-base (100M+) for PCQM4M-v2 with 25.6B tokens will take about 240 V100 GPU hours (4 V100 trained with 60 hours). Fine-tuning cost about 20 V100-hours per epoch.

For small/medium dataset, the trade-off between compute budget and performance implies that GraphGPT might not be the first choice.

However, to pursue superior performance given large amount of data, large scale GraphGPT is a very competitive candidate. Meanwhile, int8/int4-quantization techniques has been developed to allow much faster inference, even training (Dettmers et al., 2022; Frantar et al., 2022). Parallel training frameworks like DeepSpeed and Megatron enable fast mixed-precision and bf-16 precision training utilizing thousands of GPUs (Rasley et al., 2020; Shoeybi et al., 2019). Transformer-specific optimization techniques like FlashAttention-2 allows us to speed-up the training of transformer models (Dao, 2023). Last but not least, the development of GPU and tensor accelerator chips is very fast. As they are becoming much faster and cheaper, compute burden will not be a big problem.

Context window. The context window of the transformer affects the computational complexity very much. This limits the efficiency of training large (sub)graphs. Besides relying on the development of efficient training of transformers (Dao, 2023), finding short sequence representation of graphs, and exploring better ways to extract sequences from big graphs are interesting to study further.

These limitations are also opportunities that worth further explorations.